

Magnetic Resonance Tracking of Implanted Adult and Embryonic Stem Cells in Injured Brain and Spinal Cord

EVA SYKOVÁ^{a,b,c} AND PAVLA JENDELOVÁ^{a,b,c}

^a*Institute of Experimental Medicine ASCR, Prague, Czech Republic*

^b*Center for Cell Therapy and Tissue Repair, Charles University, Second Medical Faculty, Prague, Czech Republic*

^c*Department of Neuroscience, Charles University, Second Medical Faculty, Prague, Czech Republic*

ABSTRACT: Stem cells are a promising tool for treating brain and spinal cord injury. Magnetic resonance imaging (MRI) provides a noninvasive method to study the fate of transplanted cells *in vivo*. We studied implanted rat bone marrow stromal cells (MSCs) and mouse embryonic stem cells (ESCs) labeled with iron-oxide nanoparticles (Endorem®) and human CD34⁺ cells labeled with magnetic MicroBeads (Miltenyi) in rats with a cortical or spinal cord lesion. Cells were grafted intracerebrally, contralaterally to a cortical photochemical lesion, or injected intravenously. During the first week post transplantation, transplanted cells migrated to the lesion. About 3% of MSCs and ESCs differentiated into neurons, while no MSCs, but 75% of ESCs differentiated into astrocytes. Labeled MSCs, ESCs, and CD34⁺ cells were visible in the lesion on MR images as a hypointensive signal, persisting for more than 50 days. In rats with a balloon-induced spinal cord compression lesion, intravenously injected MSCs migrated to the lesion, leading to a hypointensive MRI signal. In plantar and Basso-Beattie-Bresnehan (BBB) tests, grafted animals scored better than lesioned animals injected with saline solution. Histologic studies confirmed a decrease in lesion size. We also used 3-D polymer constructs seeded with MSCs to bridge a spinal cord lesion. Our studies demonstrate that grafted adult as well as embryonic stem cells labeled with iron-oxide nanoparticles migrate into a lesion site in brain as well as in spinal cord.

KEYWORDS: cell transplantation; magnetic resonance; contrast agents; injury; photochemical lesion; spinal cord lesion

Address for correspondence: Prof. Eva Syková M.D., D.Sc., Institute of Experimental Medicine ASCR, Vídeňská 1083, 140 20 Prague 4, Czech Republic. Voice: +420-241062230; fax: +420-241062783.

sykova@biomed.cas.cz

Ann. N.Y. Acad. Sci. 1049: 146–160 (2005). © 2005 New York Academy of Sciences.
doi: 10.1196/annals.1334.014

INTRODUCTION

The adult central nervous system (CNS) possesses a limited capacity for regeneration, and the prospects for recovery after traumatic injury or ischemia or during degenerative diseases are generally grim. Stem cell research opens new possibilities for repairing the nervous system. Transplanted stem cells can either differentiate into neural cells and replace lost populations of cells or they can produce cytokines or growth factors that can lead to neural cell rescue or enhance regeneration. Considerable progress has been made in developing effective methods for culturing different types of stem cells and transplanting them into animal models of degenerative diseases, ischemia, and brain and spinal cord injury. Although the mechanisms underlying the improvements seen in cell therapy studies remain to be determined, the results are encouraging.

The stem cells can be implanted either into the site of the lesion or into the brain ventricles or they can be administered systemically (e.g., intravenously). After transplantation, the cells integrate into the host environment and respond to intrinsic signals.¹ Stem cells administered via intravenous infusion migrate only to the lesion site and enter the nervous tissue through a more permeable or opened blood–brain barrier.^{2,3}

To follow the migration and fate of implanted stem cells, the invasive analysis of brain sections post mortem has been required. Histologic methods, however, do not give us data about the dynamics of the grafting process or about the actual migration of the transplanted stem cells in the host organism. Nuclear magnetic resonance imaging (MRI) provides a noninvasive method for studying the fate of transplanted cells *in vivo* in our studies. Superparamagnetic iron-oxide nanoparticles are introduced into the cells during their cultivation prior to their grafting into the CNS tissue. The migration of transplanted adult bone marrow or embryonic stem cells can be tracked by MRI since the presence of superparamagnetic iron-oxide (SPIO) nanoparticles in the cells increases the contrast in MR images.^{4–8}

SUPERPARAMAGNETIC NANOPARTICLES USED FOR CELL LABELING

Superparamagnetic contrast agents are formed by a superparamagnetic core, which is formed by iron oxide (SPIO) crystalline structures described by the general formula $\text{Fe}_2\text{O}_3 \cdot \text{M}^{2+}\text{O}$, where M is a divalent metal ion ($\text{M} = \text{Fe}^{2+}, \text{Mn}^{2+}$). For the synthesis of the contrast agents, small crystals of magnetite Fe_3O_4 are predominantly used. During the preparation of the contrast agent, the crystals are covered by a macromolecular shell, formed by dextran, starch, and other polymers, which can be chemically or biochemically modified (FIG.1A.). On the basis of these physical properties, up to now several types of contrast agents with a nanoparticle diameter in the range of 20 to 150 nm have been described; some of them are commercially available.⁹ Different modifications of the shell (e.g., the attachment of specific antibodies) enable the contrast agent to be specifically bound to the tissue.^{9–12} For specific cell labeling, commercially available cell isolation kits for magnetic separation can also be used.^{13–15} For magnetic separation, MACS MicroBeads, which are also superparamagnetic particles that are coupled to highly specific monoclonal antibod-

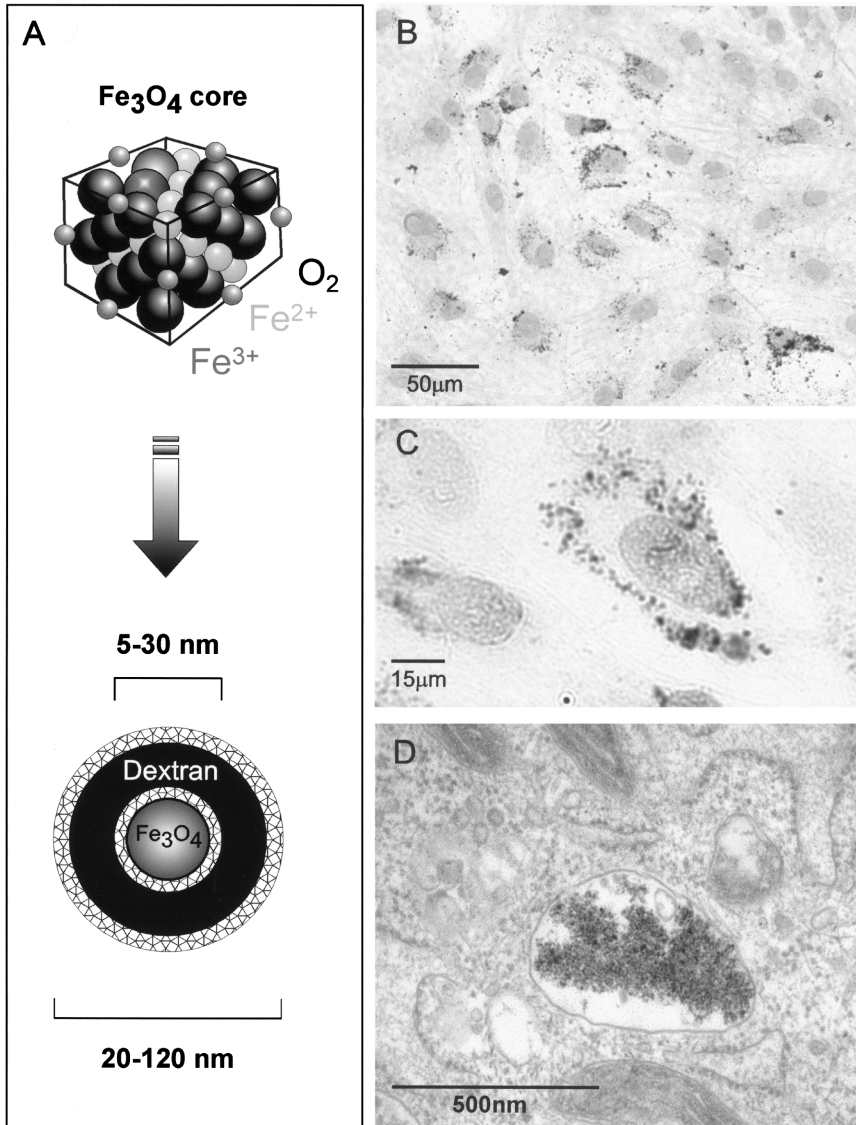


FIGURE 1. Construction of iron-oxide nanoparticles and MSC labeling with iron-oxide nanoparticles. (A) The contrast agent Endorem consists of a superparamagnetic Fe_3O_4 core that is coated by a dextran shell. (B) Cells in culture labeled with BrdU (dark nuclei), containing superparamagnetic nanoparticles (black dots). (C) A cell labeled with superparamagnetic nanoparticles undergoing cell division. (D) Transmission electron photomicrograph of a cluster of iron nanoparticles surrounded by a cell membrane. (Modified from Jendelová.⁷ From: Magnetic Resonance in Medicine. ©2003 Wiley-Liss, Inc.)

ies, are used to magnetically label the target cell population. Their diameter is approximately 50 nm in size, which is comparable to the nanoparticle diameter of commonly used superparamagnetic MR contrast agents.

Nanoparticles based on magnetite are characterized by superparamagnetism, which occurs when crystal-containing regions with unpaired spins are sufficiently large that they can be regarded as thermodynamically independent, single-domain particles. The application of a nanoparticle contrast agent in MRI leads to a shortening of both T1 and T2 relaxation times that is one or two orders of magnitude greater than that seen with standard paramagnetic contrast. Thus, it is possible to observe changes in contrast on the cellular level by mini- and microimaging MR techniques.

Nanoparticles can be taken up by cells during cultivation by endocytosis,^{7,8} although different methods to facilitate entry are often required (e.g., lipofection, transfection agents, antibody–iron oxide particle constructs^{4,16,17}). In tissue the cells can be detected either by staining for iron to produce ferric ferrocyanide (prussian blue) or by one of a number of widely used labeling methods employed prior to transplantation (bromodeoxyuridine [BrdU], green fluorescent protein [GFP], or lacZ^{2,7,18–21}).

IMPLANTATION OF MSCs IN RATS WITH A CORTICAL PHOTOCHEMICAL LESION

Marrow stromal cells (MSCs) isolated from bone marrow are multipotent progenitor cells and can differentiate in culture into osteoblasts, chondrocytes, adipocytes and myoblasts.²² After transplantation into the brain, MSCs respond to intrinsic signals and differentiate *in vivo* into astrocytes, microglia, and even neurons.¹⁹ The use of MSCs in cell therapies may have some advantages over the use of other sources of cells: they are relatively easy to isolate (from bone marrow), they may be used in autologous transplantation protocols, and bone marrow as a source of cells has already been approved for the treatment of hematopoietic diseases. Various routes of administration of MSCs have been tested. Kopen *et al.*¹⁹ injected MSCs into the lateral ventricle, and these cells migrated throughout the forebrain and cerebellum including the striatum, the molecular layer of the hippocampus, the olfactory bulb, and the internal granular layer of the cerebellum. Li *et al.*³ and Lu *et al.*² transplanted MSCs either directly into the striatum and cortex or intravenously into rats exposed to brain injury and focal cerebral ischemia. These cells migrated from the injection site and traveled to the boundary zone of the injury and the corpus callosum.

For the isolation of rat MSCs, femurs were dissected from 4-week-old Wistar rats. Marrow cells were plated on 80 cm² tissue culture flasks in DMEM/10% FBS with 100 U/mL penicillin and 100U/mL streptomycin. After 24 hours, the non-adherent cells were removed by replacing the medium. The medium was replaced every 2–3 days as the cells grew to confluence. After 6 to 10 passages, superparamagnetic dextran-coated iron-oxide nanoparticles, commercially known as Endorem (Guerbet, Roissy, France; 2.2 mg of iron), were added to the culture of rat MSCs 5 days prior to transplantation. After 72 hours the contrast agent was washed out and the cells were co-labeled with BrdU. Since BrdU is incorporated only into proliferating cells, double-staining for BrdU and prussian blue (staining for iron) shows that iron-oxide containing cells are viable. (FIG. 1B and C). Transmission electron microscopy confirmed the

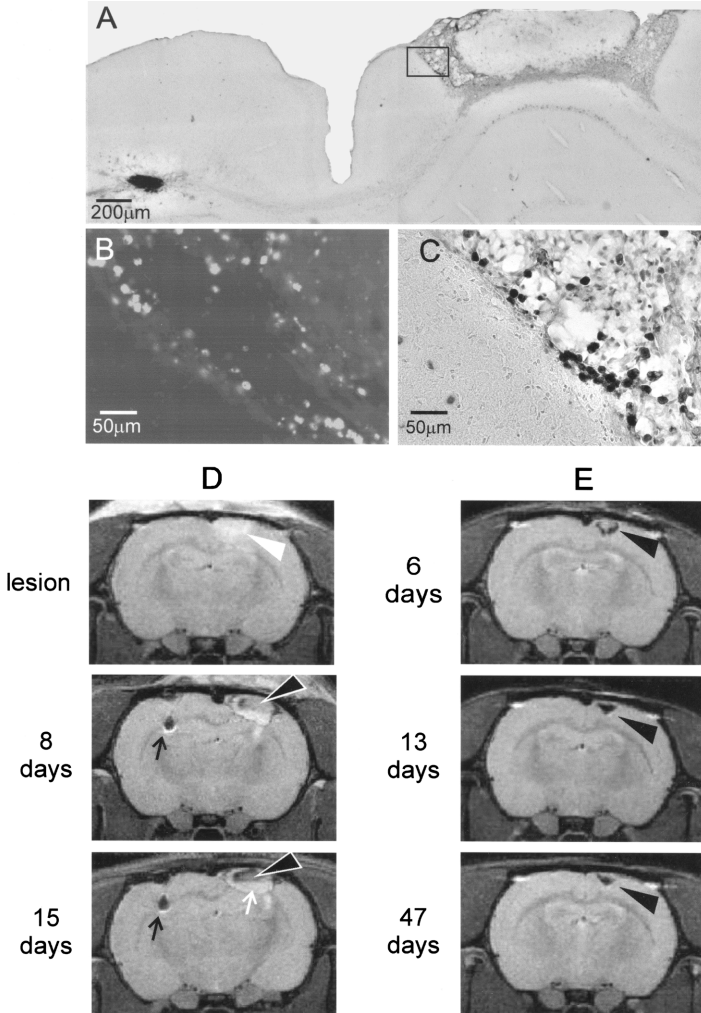


FIGURE 2. Implantation of MSCs into brains with photochemical lesions. (A) Prussian blue staining of an injection site in the contralateral hemisphere and a photochemical lesion 4 weeks after grafting. (B) Higher-magnification photomicrograph of anti-BrdU staining showing BrdU-positive MSCs in the lesion and (C) prussian blue-stained MSCs along the left edge of the photochemical lesion. (D) MR images of a cortical photochemical lesion and MSCs implanted into the contralateral hemisphere. A photochemical lesion (*white arrowhead*) 12 hours after thrombosis and prior to any cell implantation. The cell implant (*black arrow*) in the hemisphere contralateral to the lesion is seen as a hypointensive area, while the lesion (*black arrowheads*) is visible as a hypointensive signal 8 days after grafting and is further enhanced at day 15. (E) MR images of a cortical photochemical lesion and MSCs injected into the femoral vein. A hypointensive signal (*black arrowhead*) observed 6 days after intravenous injection was further enhanced at day 13 post injection and persisted for 47 days. (Modified from Jendelová.⁷ From: *Magnetic Resonance in Medicine*. ©2003 Wiley-Liss, Inc.)

presence of 20–50 iron-oxide particles inside the cell, observed as membrane-bound clusters within the cell cytoplasm (FIG. 1D).

Endorem/BrdU co-labeled MSCs were grafted into rats with a cortical photochemical lesion (FIG. 2A).⁷ Two weeks after implantation the cells massively populated the border zone of the damaged cortical tissue and were localized in the injured tissue around the necrotic part of the photochemical lesion (FIG. 2B and C). Only few (less than 3%) of the cells that migrated into the lesion expressed the neuronal marker NeuN when tested 28 days post implantation. No GFAP-positive cells were found in the lesion.

Rats with grafted Endorem/BrdU co-labeled cells were examined weekly for a period of 3–7 weeks post transplantation using a 4.7 T Bruker spectrometer. Single sagittal, coronal, and transversal images were obtained by a fast gradient echo sequence for localizing subsequent T₂-weighted transversal images measured by a standard turbo spin echo sequence. The lesion was clearly visible on MR images 2 hours after light exposure as a hyperintense signal (FIGS. 2D and 3A) and remained visible during the entire measurement period. No recognizable hypointense signal in the lesion was detected during the first 2 days after implantation. A decrease in MR signal was found only at the injection site in animals with cells injected contralaterally to the lesion. One week after grafting, we observed a hypointense signal in the lesion, which intensified during the second and third weeks (FIG. 2D). Histologic study confirmed that a large number of prussian blue-positive cells had entered the lesion. No hypointense signal was found in other brain regions. The hypointense signal occurred only in damaged areas populated with MSCs, and its intensity corresponded to prussian blue or BrdU staining.

After the intravenous injection of MSCs, we found a similar hypointense MR signal in the lesion site. The signal was observed 6 days after cell infusion and persisted for 7 weeks (FIG. 2E). Prussian blue and anti-BrdU staining confirmed the presence of iron-oxide-BrdU co-labeled cells in the lesion, which densely populated the borders of the lesion.

Only a few cells weakly stained for prussian blue were found in photochemical lesions without any implanted cells (FIG. 3D). The staining represents iron, which most likely originated in hemorrhages and iron degradation products released from iron-containing proteins (such as hemoglobin, ferritin and hemosiderin) and phagocytized by microglia/macrophages. We did not observe any BrdU-positive cells in the brains of non-grafted animals.

To mimic the signal behavior in brain tissue, we performed *in vitro* imaging of labeled cells. Rat MSCs were labeled with Endorem as described above, and a cell suspension (at concentrations of 10,000; 5000; 2500; 1250; 625 or 315 cells per μL) was suspended in 1.7% gelatin. MR images showed a hypointense signal at all concentrations above 625 cells per liter, meaning that contrast changes are visible when approximately 70 or more cells are in the image voxel.⁷

IMPLANTATION OF EMBRYONIC STEM CELLS

Embryonic stem cells (ESCs) are undifferentiated pluripotent cells derived from the inner cell mass of blastocyst-stage embryos. They maintain a normal karyotype and they can be propagated *in vitro* indefinitely in the primitive embryonic state.

ESCs can, by definition, give rise to any cell type in the body, including germ cells. Mouse ES cell-derived glial precursors, transplanted into a rat with myelin disease, interact with the host neurons to produce myelin in the brain and spinal cord.²⁴ Retinoic acid-treated embryoid bodies from mouse ESCs, when transplanted into a rat spinal cord 9 days after traumatic injury, differentiated into astrocytes, oligodendrocytes, and neurons and promoted recovery.²⁵ Bjorklund *et al.*²⁶ reported that undifferentiated mouse ESCs can become dopamine-producing neurons in the brain in a rat model of Parkinson's disease and can lead to partial functional recovery.

We used mouse D3 ESCs transfected with the pEGFP-C1 vector. Since undifferentiated ESCs may form embryonic tumors when grafted into a host animal, we induced neural differentiation by culturing eGFP ESCs in serum containing DMEM/F12 without LIF for 2 days and then transferring the cells into serum-free media supplemented with insulin, transferrin, selenium, and fibronectin for further culture. Feeder-free eGFP ESCs were labeled with Endorem (112.4mg/mL). Transplanted cells were detected by staining for iron and by GFP fluorescence. Cells were transplanted intracerebrally or intravenously on the 8th day of differentiation into adult Wistar rats with a cortical photochemical lesion.⁸ When we implanted ESCs 7 days post lesion, we found a massive migration of Endorem-labeled GFP-positive cells into the lesion site regardless of the route of administration (direct injection into the contralateral hemisphere or intravenous injection; FIGS. 3E and F). In rats with a photochemical lesion and contralaterally injected cells, the cell implants were clearly visible on MR images as a hypointense area at the injection site (FIG. 3B). Two weeks after grafting, a hypointense signal was also observed in the corpus callosum. At the same time, histologic study showed that a large number of prussian blue-positive cells had entered the lesion. Many labeled cells were also detected in the corpus callosum, suggesting a migration from the contralateral hemisphere towards the lesion.

When the ESCs were injected intravenously into lesioned rats, we found a hypointense MRI signal only at the site of the lesion (FIG. 3C). The first changes in the hypointensity of the MRI signal in the lesion were observed 1 week after cell injection. The hypointense signal in the lesion reached its maximum at about 2 weeks and persisted with no apparent decrease in signal intensity for the rest of the measurement period (5 weeks). Of all the eGFP ESCs containing nanoparticles found in the lesion, 70% of them were astrocytes, very few (less than 1%) were oligodendrocytes, and about 5% of nanoparticle-labeled eGFP ESCs had differentiated into neurons.⁸

IMPLANTATION OF CD34⁺ CELLS

CD34⁺ cells—a subset of bone marrow cells—are known as hematopoietic progenitor cells.²⁷ These cells can be purified using a Miltenyi MACS sorter and clinically used for hematopoiesis restoration.^{13–15} In addition, hematopoietic progenitors express neural genes,²⁸ and therefore they may be a potential resource for generating neural stem cells in order to treat defects in the injured CNS. The CD34⁺ cells are separated by means of immunomagnetic selection with anti-CD34 antibodies. For sorting, MicroBeads with a superparamagnetic iron-oxide core coated with a polysaccharide that is linked to an antibody are bound to the respective cell. The selected CD34⁺ cells retain the magnetic label attached to their surface, and since the

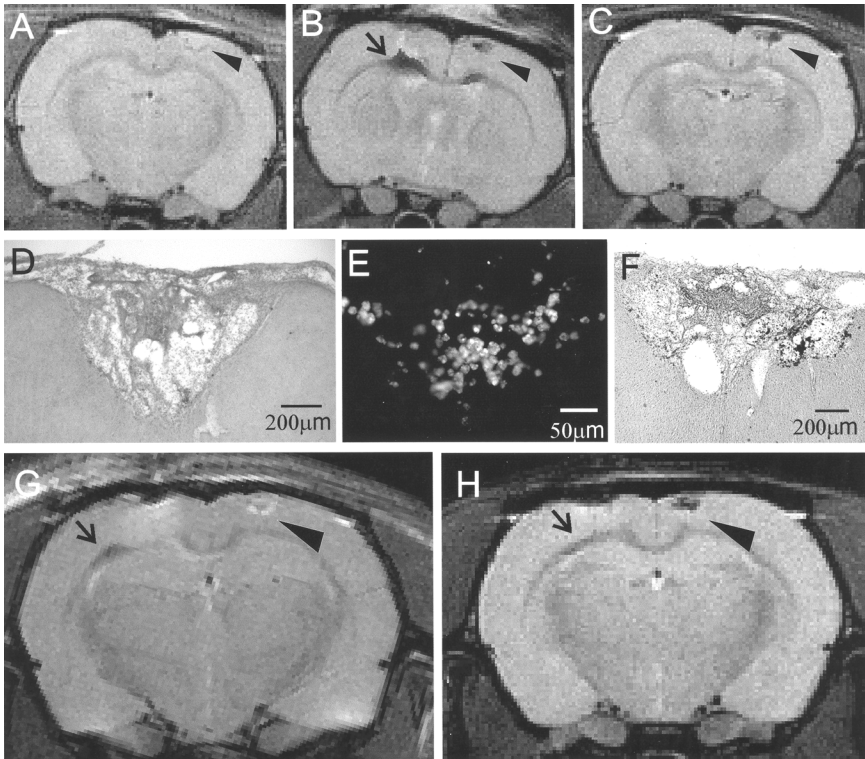


FIGURE 3. A cortical photochemical lesion and implanted eGFP ESCs or CD34⁺ cells. (A) A cortical photochemical lesion (*arrowhead*) visible on MR images two weeks after induction as a hyperintensive area with sharp hypointensive borders. (B) Both the cell implant of eGFP ESCs (in the hemisphere contralateral to the lesion; *arrow*) and the lesion (*arrowhead*) are hypointense in MR images 2 weeks after implantation. (C) A hypointensive signal in the lesion (*arrowhead*) 2 weeks after the intravenous injection of nanoparticle-labeled eGFP ESCs. (D) A few cells weakly stained for prussian blue were found in the photochemical lesion in animals without implanted cells. (E) Higher-magnification photomicrograph of GFP-labeled cells showing GFP-positive ESCs in the lesion. (F) Massive invasion of prussian blue-stained cells into the lesion 4 weeks after the intravenous injection of eGFP ESCs. (G) A cell implant of CD34⁺ cells (in the hemisphere contralateral to the lesion; *arrow*) visible as a hypointensive area in MR images 24 hours post injection; the lesion (*arrowhead*) remained hyperintensive. (H) A hypointensive signal in the lesion (*arrowhead*) 4 weeks after grafting. (A–F modified from Jendelová.⁸ From: *Journal of Neuroscience Research* ©2004 Wiley-Liss, Inc.)

size of the MicroBeads' superparamagnetic core is comparable to the size of the superparamagnetic core of MR contrast agents (Endorem), MicroBeads provide sufficient contrast on MR images.²⁹

Human cells from peripheral blood were selected by CliniMACS CD34 Selection Technology (Miltenyi). The CliniMACS is an automated cell selection device, based on MACS Technology. It enables the operator to perform large-scale magnetic cell selection in a closed and sterile system. Before selection the cells are magnetically labeled using a cell type-specific reagent. We first determined that after cryopreservation, the Microbeads remain bound to the cell surface. Transmission electron microscopy confirmed the presence of several iron-oxide nanoparticles attached to the cell surface. Iron content after mineralization was measured by spectrophotometry. The average iron content per cell was 0.275 pg. This value is lower by an order of magnitude than in the case of cell labeling using Endorem or other contrast agents that enter the cell (17 pg).⁷

Purified CD34⁺ cells were implanted into rats with a cortical photochemical lesion, contralaterally to the lesion.²⁹ Twenty-four hours after grafting, the implanted cells were detected in the contralateral hemisphere as a hypointense area on T2W images (FIG 3G); the hypointensity of the implant decreased during the first week. At the lesion site we observed a hypointensive signal 10 days after grafting that persisted for the next 3 weeks, until the end of the experiment (FIG. 3H). Prussian blue and anti-human nuclei staining confirmed the presence of magnetically labeled human cells in the corpus callosum and in the lesion 4 weeks after grafting. CD34⁺ cells were also found in the subventricular zone (SVZ). Human DNA (a human-specific 850-base-pair fragment of α -satellite DNA from human chromosome 17) was detected in brain tissue sections from the lesion using PCR, confirming the presence of human cells.²⁹ This is the first study showing that CD34 MicroBeads superparamagnetic nanoparticles can be used as a magnetic cell label for *in vivo* cell visualization.

IMPLANTATION OF MSCs INTO RATS WITH A SPINAL CORD COMPRESSION LESION

Severe injury of the spinal cord results in the formation of a complex lesion. The center of the lesion is necrotic, which later often results in the formation of a cyst, and the lesion is surrounded by a scar that consists of reactive astrocytes producing extracellular matrix proteins (chondroitin sulfate proteoglycans³⁰). This environment prevents regenerating axons from transversing the lesion. Since it was shown by Maysinger *et al.*³¹ that bone marrow cells secrete interleukins, stem cell factor and hematopoietic cytokine colony-stimulating factor-1 (which is a growth factor in the central nervous system) MSCs transplanted into the injured CNS could potentially stimulate tissue regeneration and promote the recovery of function and improve neurological deficits by mechanisms other than direct neuronal replacement. We therefore studied lesion size, the functional effects of cell transplantation and the fate of MSCs transplanted into rats with a spinal cord injury.

As a model of spinal cord injury we used a balloon-induced compression lesion.³² A 2-French Fogarty catheter is inserted into the dorsal epidural space through a small hole made in the Th10 vertebral arch. A spinal cord lesion is made by balloon

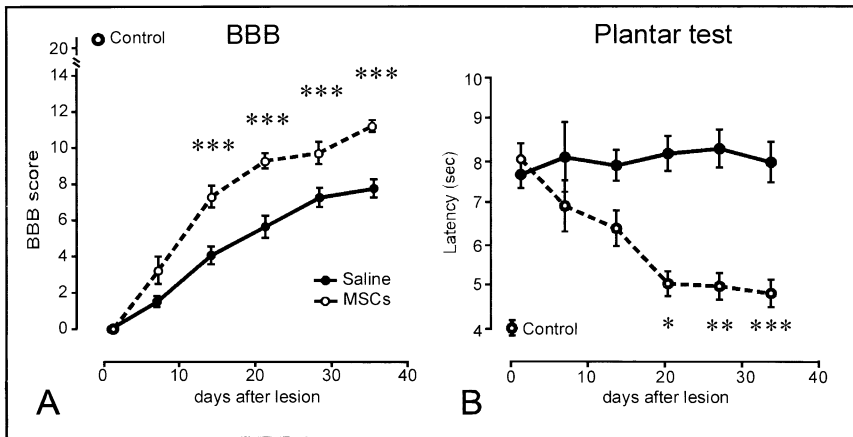


FIGURE 4. Behavioral testing of rats with spinal cord lesion. (A) BBB scores are significantly higher in rats with implanted MSCs than in saline-injected rats. (B) The sensitivity of the hind limbs is expressed by the plantar score, which is significantly higher in rats treated with MSCs.

inflation (volume 15 μ L) at the Th8–Th9 spinal level. Inflation for 5 minutes produces paraplegia and is followed by gradual recovery.

MSCs labeled with Endorem were injected intravenously into the femoral vein one week after lesioning.⁸ MR images were taken *ex vivo* 4 weeks after cell implantation using a standard whole-body resonator. Functional status was assessed weekly for 5 weeks after spinal cord lesioning, using the Basso–Beattie–Bresnehan (BBB) locomotor rating score and the plantar test. Our data indicate that lesioned animals with grafted MSCs have higher locomotor scores as indicated by their BBB scores and show better responses in the plantar test than do control animals (FIG. 4). Particularly, the plantar test shows the recovery of sensitivity in the hind limbs. On MR images we observed the lesion as an inhomogeneity in the tissue texture with a hypointense signal only in the area of the spinal channel (FIGS. 5A and C). Images of longitudinal as well as transversal spinal cord sections from animals grafted with magnetically labeled MSCs showed the lesion as a dark hypointense area (FIGS. 5B and D). Prussian blue staining confirmed a large number of positive cells present in the lesion. Compared to control rats, in grafted animals the lesion, which was populated by grafted MSCs, was considerably smaller, suggesting the possibility of a positive effect of the MSCs on lesion repair (FIGS. 5E and F).

HYDROGELS AND CELL–POLYMER CONSTRUCTS

Since CNS injury (particularly spinal cord injury) is accompanied by cellular death and glial scar formation that affects regeneration in the injured region, extensive research is being done to prevent scarring and to bridge the lesion. Macroporous

biocompatible hydrogels can be used to eliminate scarring and to facilitate regeneration.^{33,34} These hydrogels are highly biocompatible, and when implanted into nervous tissue they are known to be chemically inert and nontoxic.³⁵ They have a high water content (70–90%) and a very large surface area, and they are macroporous with pore sizes of 10–50 μm .

Hydrogel implantation can be combined with stem cell grafting. Before transplantation into the lesion, the hydrogels can be seeded with stem cells. In this case the hydrogels form an inert environment, allowing for the free diffusion of intrinsic growth factors, in which the cells start to differentiate and migrate. The inert environment in the hydrogels also provides an adequate standard background for MR imaging of the cells. In our studies we employed cell–polymer constructs in order to facilitate the regeneration of injured spinal cord. The scaffold of the cell–polymer constructs was made of non-resorbable biocompatible macroporous hydrogels based on copolymers of 2-hydroxyethylmethacrylate (HEMA) with communicating pores. This scaffold was seeded with Endorem-labeled MSCs (FIG. 5G). The cells migrated from the medium into the central zone of the hydrogel blocks, proving that *in vitro* the MSCs are able to move through the communicating pores of the hydrogels.^{35,36}

The cells survived in the hydrogels for four weeks. The diffusion parameters of the cell–polymer constructs were determined by the TMA⁺ real-time ionophoretic method using ion-selective microelectrodes.^{37,38} The volume fraction represents the space between the structural components of the hydrogel, and the gel provides in-growing cells with mechanical stability and a large surface area. The tortuosity, representing the TMA⁺ molecule paths, is low in the hydrogels, since diffusion in the hydrogels is not hindered as it is in the adult CNS, particularly in injured regions.³⁹ The growth of MSCs in hydrogels *in vitro* did not lead to decreased diffusion in the hydrogels, and thus diffusion in the cell–polymer constructs is not hindered and allows for the free diffusion of neurotransmitters or growth factors.³⁶

To evaluate the ability of cell–polymer constructs to bridge a lesion, we removed the right half of a spinal cord segment by hemisection and inserted a block of HEMA hydrogel seeded with Endorem-labeled MSCs.⁴⁰ Six weeks after implantation, the hydrogel had formed a continuous bridge between the hemisected spinal segments, re-establishing the anatomical continuity of the tissue. The hydrogel was visible on MRI as a hypointense area (FIG. 5H) and prussian blue staining confirmed positively stained cells within the hydrogel. Staining for neurofilaments (NF160 Sigma, St. Louis, MO, USA) showed axonal ingrowth into the hydrogel. Hydrogels seeded with stem cells may therefore serve as an alternative to the conventional grafting of dissociated cells, benefiting from advances in surface chemistry and the cell–cell or cell–matrix interactions that occur during development or regeneration.

FURTHER PERSPECTIVES AND CONCLUSIONS

MRI techniques can be used to monitor the fate of transplanted stem cells in a host organism. Both rat marrow stromal cells and mouse embryonic stem cells were labeled *in vitro* with superparamagnetic nanoparticles and implanted into the brain or spinal cord of rats. The distribution of the labeled cells can be monitored at regular intervals after implantation by MRI. Moreover, MicroBeads superparamagnetic

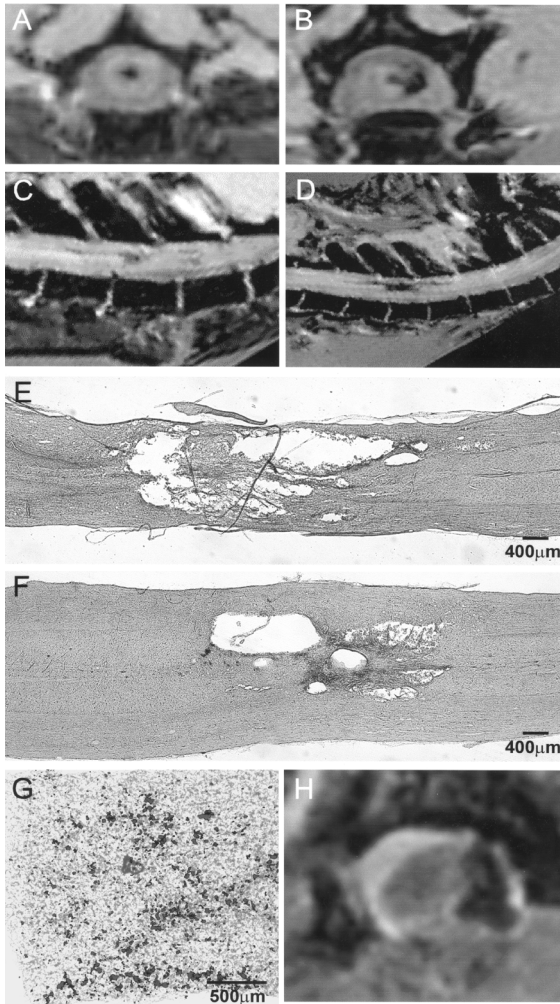


FIGURE 5. MSCs labeled with nanoparticles implanted into rats with a spinal cord compression lesion. (A,C) Transversal and longitudinal sections of a spinal cord compression lesion on *ex vivo* MR images 5 weeks after compression. The lesion is seen as a hyperintensive area with a weak hypointensive signal in the spinal cord channel within the lesion. (B,D) Transversal and longitudinal images of a spinal cord compression lesion populated with intravenously injected nanoparticle-labeled MSCs 4 weeks after implantation. The lesion with nanoparticle-labeled cells is visible as a dark hypointensive area. (E) Prussian blue staining of a spinal cord compression lesion (control animal). (F) Prussian blue staining of a spinal cord lesion with intravenously injected nanoparticle-labeled MSCs. The lesion is populated with prussian blue-positive cells. Note the smaller lesion size in the implanted animal than in the control. (G) Endorem-labeled cells seeded into a hydrogel. (H) On MR images 6 weeks after implantation, the hydrogel was visible as a hypointensive area. (A–F modified from Jendelová.⁸ From: *Journal of Neuroscience Research*. © 2004. Wiley-Liss, Inc.)

nanoparticles, used for specific magnetic sorting, can also be used as a magnetic cell label for *in vivo* cell visualization with MRI. Using MicroBeads, about 450 labeled cells are needed for MRI detection since the average iron content per cell is lower by an order of magnitude than in the case of intracellular contrast agents such as Endorem, where 70 cells are needed.

This MR technique gives us information about the migration speed of the transplanted cells towards a brain or spinal cord lesion and about their fate in CNS tissue. The obtained data from MR were correlated with histologic and electron microscopy findings. These correlations significantly contributed to our knowledge about the dynamics of the transplanted stem cells in the host organism. In the future, the described methodology would enable us to follow the migration of transplanted cells in humans, establish the optimal number of transplanted cells, define therapeutic windows, and monitor cell growth and possible side effects (malignancies). Currently, the described immunolabeling of specific cell types with clinically approved MicroBeads may help to elucidate the fate of implanted stem cells and evaluate the effect of cell therapy in patients with various diseases and brain or spinal cord injury.

However, in the case of large lesions, cells are not able to repair the tissue. It is necessary to fill the gap left by the lost cell population in order to provide support for tissue restoration, reduce the glial scar, and create a permissive environment for cellular ingrowth. Biocompatible non-resorbable polymer hydrogels, based on pHEMA, are suitable implantation materials used in medicine, and the implantation of these hydrogels can reduce scar tissue formation and bridge a lesion, creating an environment permissive for cellular ingrowth and the diffusion of various neuroactive substances, including growth factors.⁴¹ These hydrogels are in many ways similar to the environment in developing nervous tissue³⁵ and can mechanically support the ingrowing cells and axons. In addition, their chemical and physical properties can be tailored to a specific use, and the gels can be seeded with different types of stem cells creating cell-polymer constructs.

At the present time we have to take into consideration all necessary precautions before the practical employment of cell therapy in patients suffering from degenerative diseases of the CNS or in patients with severe traumatic lesions of the CNS can be realized. While the use of a patient's autologous (adult) stem cells will probably not have serious complications, current experiments with embryonic stem cells do not give us enough information about the behavior of the transplanted cells in the host organism, especially about their influence outside the target structures and their potential neoplastic growth.

Animal studies indicate that improved neural functioning can result from bone marrow stem cell transplantation.^{2,8,20,21,23} Therefore cell therapy has started to be used in patients suffering from brain and spinal cord injury. On the basis of our experimental studies, autologous bone marrow mononuclear cell implantation is being used in our Phase I clinical study in patients with transversal spinal cord lesions (Autologous Transplantation of Bone Marrow Cells into Patients with Transversal Spinal Cord Injury, coordinator E. Syková). At this time we can conclude that implantation is safe, as there were no complications following intravenous or intra-arterial administration into 9 acute and 9 chronic patients. We are using MEP, SEP, MRI, and the Asia score in our patient follow-up. Although partial improvement was observed in acute patients, further evaluation of a much larger population of patients is needed before any conclusions can be made.

REFERENCES

1. ROSARIO, C.M. *et al.* 1997. Differentiation of engrafted multipotent neural progenitors towards replacement of missing granule neurons in meander tail cerebellum may help determine the locus of mutant gene action. *Development* **124**: 4213–4224.
2. LU, D. *et al.* 2001. Adult bone marrow stromal cells administered intravenously to rats after traumatic brain injury migrate into brain and improve neurological outcome. *Neuroreport* **12**: 559–563.
3. NAKANO, K. *et al.* 2001. Differentiation of transplanted bone marrow cells in the adult mouse brain. *Transplantation* **71**: 1735–1740.
4. BULTE, J.W. *et al.* 1999. Neurotransplantation of magnetically labeled oligodendrocyte progenitors: magnetic resonance tracking of cell migration and myelination. *Proc. Natl. Acad. Sci. USA* **96**: 15256–15261.
5. BULTE, J.W. *et al.* 2001. Magnetodendrimers allow endosomal magnetic labeling and in vivo tracking of stem cells. *Nat. Biotechnol.* **19**: 1141–1147.
6. HOEHN, M. *et al.* 2002. Monitoring of implanted stem cell migration in vivo: A highly resolved in vivo magnetic resonance imaging investigation of experimental stroke in rat. *Proc. Natl. Acad. Sci. USA* **100**: 1073–1078.
7. JENDELOVÁ, P. *et al.* 2003. Imaging the fate of implanted bone marrow stromal cells labeled with superparamagnetic nanoparticles. *Magn. Reson. Med.* **50**: 767–776.
8. JENDELOVÁ, P. *et al.* 2004. MR tracking of transplanted bone marrow and embryonic stem cells labeled by iron oxide nanoparticles in rat brain and spinal cord. *J. Neurosci. Res.* **76**: 232–243.
9. WANG, Y.X., S.M. HUSSAIN & G.P. KRESTIN. 2001. Superparamagnetic iron oxide contrast agents: physicochemical characteristics and applications in MR imaging. *Eur. Radiol.* **11**: 2319–2331.
10. WEISSLEDER, R. *et al.* 1997. Magnetically labeled cells can be detected by MR imaging. *J. Magn. Reson. Imaging* **7**: 258–263.
11. YEH, T. *et al.* 1993. Intracellular labeling of T-cells with superparamagnetic contrast agents. *Magn. Reson. Med.* **30**: 617–625.
12. YEH, T. *et al.* 1995. In vivo dynamic MRI tracking of rat T-cells labeled with superparamagnetic iron-oxide particles. *Magn. Reson. Med.* **33**: 200–208.
13. LANG, P. *et al.* 2003. Transplantation of highly purified CD34+ progenitor cells from unrelated donors in pediatric leukemia. *Blood* **101**: 1630–1636.
14. HANDGRETINGER, R. *et al.* 2002. Isolation and transplantation of highly purified autologous peripheral CD34(+) progenitor cells: purging efficacy, hematopoietic reconstitution and long-term outcome in children with high-risk neuroblastoma. *Bone Marrow Transplant.* **29**: 731–736.
15. HANDGRETINGER, R. *et al.* 2001. Megadose transplantation of purified peripheral blood CD34(+) progenitor cells from HLA-mismatched parental donors in children. *Bone Marrow Transplant.* **27**: 777–783.
16. ARBAB, A.S. *et al.* 2003. Characterization of biophysical and metabolic properties of cells labeled with superparamagnetic iron oxide nanoparticles and transfection agent for cellular MR imaging. *Radiology* **229**: 838–846.
17. FRANK, J.A. *et al.* 2002. Magnetic intracellular labeling of mammalian cells by combining (FDA-approved) superparamagnetic iron oxide MR contrast agents and commonly used transfection agents. *Acad Radiol. (Suppl. 2)* **9**: S484–487.
18. BRAZELTON, T.R. *et al.* 2000. From marrow to brain: expression of neuronal phenotypes in adult mice. *Science* **290**: 1775–1779.
19. KOPEN, G.C., D.J. PROCKOP & D.G. PHINNEY. 1999. Marrow stromal cells migrate throughout forebrain and cerebellum, and they differentiate into astrocytes after injection into neonatal mouse brains. *Proc. Natl. Acad. Sci. USA* **96**: 10711–10716.
20. LU, D., *et al.* 2001. Intraarterial administration of marrow stromal cells in a rat model of traumatic brain injury. *J. Neurotrauma* **18**: 813–819.
21. SASAKI, M., *et al.* 2001. Transplantation of an acutely isolated bone marrow fraction repairs demyelinated adult rat spinal cord axons. *Glia* **35**: 26–34.
22. PROCKOP, D.J. 1997. Marrow stromal cells as stem cells for nonhematopoietic tissues. *Science*. **276**: 71–74.

23. LI, Y. *et al.* 2001. Treatment of stroke in rat with intracarotid administration of marrow stromal cells. *Neurology*. **56**: 1666–1672.
24. BRUSTLE, O. 1999. Building brains: neural chimeras in the study of nervous system development and repair. *Brain Pathol.* **9**: 527–545.
25. McDONALD, J.W. *et al.* 1999. Transplanted embryonic stem cells survive, differentiate and promote recovery in injured rat spinal cord. *Nat. Med.* **5**: 1410–1412.
26. BJORKLUND, L.M. *et al.* 2002. Embryonic stem cells develop into functional dopaminergic neurons after transplantation in a Parkinson rat model. *Proc. Natl. Acad. Sci. USA*. **99**: 2344–2349.
27. CIVIN, C.I. & S.D. GORE. 1993. Antigenic analysis of hematopoiesis: a review. *J. Hematother.* **2**: 137–144.
28. GOOLSBY, J. *et al.* 2003. Hematopoietic progenitors express neural genes. *Proc. Natl. Acad. Sci. USA* **100**: 14926–14931.
29. JENDELOVÁ, P., *et al.* MR tracking of human CD34+ progenitor cells separated by means of immunomagnetic selection and transplanted into injured rat brain. *Cell Transplant.* In press.
30. BECKER, D., C.L. SADOWSKY & J.W. McDONALD. 2003. Restoring function after spinal cord injury. *Neurologist* **9**: 1–15.
31. MAYSINGER, D., O. BEREZOVSKAYA & S. FEDOROFF. 1996. The hematopoietic cytokine colony stimulating factor 1 is also a growth factor in the CNS. II. Microencapsulated CSF-1 and LM-10 cells as delivery systems. *Exp. Neurol.* **141**: 47–56.
32. VANICKY, I., *et al.* 2001. A simple and reproducible model of spinal cord injury induced by epidural balloon inflation in the rat. *J. Neurotrauma* **18**: 1399–1407.
33. WOERLY, S. *et al.* 1998. Heterogeneous PHPMA hydrogels for tissue repair and axonal regeneration in the injured spinal cord. *J. Biomater. Sci. Polym. Ed.* **9**: 681–711.
34. WOERLY, S. *et al.* 2001. Reconstruction of the transected cat spinal cord following NeuroGel implantation: axonal tracing, immunohistochemical and ultrastructural studies. *Int. J. Dev. Neurosci.* **19**: 63–83.
35. LESNY, P. *et al.* 2002. Polymer hydrogels usable for nervous tissue repair. *J. Chem. Neuroanat.* **23**: 243–247.
36. LESNY, P. *et al.* 2004. Macroporous hydrogels based on 2-hydroxyethyl methacrylate. Part 4: Growth of rat bone marrow stromal cells in three-dimensional hydrogels with positive and negative surface charges and in polyelectrolyte complexes. *J. Mater. Sci.: Mater. Med.* In press.
37. NICHOLSON, C. & E. SYKOVA. 1998. Extracellular space structure revealed by diffusion analysis. *Trends Neurosci.* **21**: 207–215.
38. SYKOVÁ, E. 1997. Extracellular space volume and geometry of the rat brain after ischemia and central injury. *Adv. Neurol.* **73**: 121–135.
39. SYKOVÁ, E. 2004. Diffusion properties of the brain in health and disease. *Neurochem. Int.* **45**: 453–466.
40. JENDELOVÁ, P. *et al.* 2004. Hydrogel implantation into a spinal cord lesion: an alternative to conventional cell grafting. Program No. 106.13.2004. Abstract Viewer/Itinerary Planner <<http://sfn.scholarone.com/itin2004/index.html>>.
41. WOERLY, S. *et al.* 1999. Neural tissue formation within porous hydrogels implanted in brain and spinal cord lesions: ultrastructural, immunohistochemical, and diffusion studies. *Tissue Eng.* **5**: 467–488.